Antenna Diversity in Multiuser Data Networks

Jing Jiang, *Student Member, IEEE*, R. Michael Buehrer, *Member, IEEE*, and William H. Tranter, *Fellow, IEEE*

***Abstract*—We consider the use of multiple antennas at the transmitter and/or the receiver to provide open-loop spatial diversity in a multiuser wireless data network. With channel quality information (CQI) available to the transmitter, and by always scheduling the transmission to the active user having the best channel conditions at the time of scheduling, another form of diversity, termed multiuser diversity, is obtained in a data system. This paper provides an analysis of the interaction between these two forms of diversity. From a network point of view, we prove that the asymptotic sum rate, in the limit of a large number of active homogeneous users and subject to the same average total transmit power, is inversely related to the number of transmit antennas for independent and identically distributed (i.i.d.) flat Rayleigh fading channels. In the case of i.i.d. flat Rician fading, the asymptotic sum rate also depends inversely on the number of transmit antennas, but directly on the number of receive antennas. Numerically, we show that the total diversity gain is also constrained by finite CQI quantization and channel fading statistics.**

***Index Terms*—Antenna arrays, diversity methods, multiuser diversity, scheduling, signal-to-noise ratio (SNR) quantization.**

I. Introduction

THE use of multiple antennas to provide antenna diversity over a point-to-point wireless link has been studied extensively since the early 1960s. It is still a popular research topic for improving energy efficiency through the use of both transmit and receive diversity. Recently, with the increasing demand for high-speed wireless data services, antenna diversity in a multiuser data network has received particular attention [1], [2], as it requires a broader multilink perspective for the spatial diversity gain in the system [3]. Recent progress in information theory [4], [5] has shown that in a data network with multiple active users requesting services simultaneously, multiuser diversity can be obtained by a packet scheduler at the medium-access control (MAC) layer, which always allocates the common radio resource to the user having the best channel quality, on the condition that the instantaneous user channel quality information (CQI) in terms of signal-to-noise ratio (SNR) is available to the scheduler. In this paper, we refer to this multiuser scheduling scheme as greedy scheduling. In fact, from a network perspective, both antenna diversity and multiuser diversity can be thought of as spatial diversity in different forms. The latter can be viewed as selection transmit diversity, with multiple users being treated as additional antennas, under the assumption that the channel fading is independent across multiple antennas and among different users. This multiuser system point of view also leads us to consider the interaction among these different forms of spatial diversity and to search for the best combination for maximizing the achievable system throughput.

With a single transmit and a single receive antenna, the total system throughput is maximized under the greedy scheduling algorithm. Further, this greedy radio resource allocation is optimal in terms of total throughput in both a multiple-access channel [4] and a parallel Gaussian broadcast channel [5]. Without loss of generality, we focus on the downlink of a cellular system with time-slotted and single-stream transmission over each time slot. A practical channel-aware scheduling algorithm, proportional fair (PF) scheduling [3], [6], has been used in the downlink of cellular packet data system IS-856 [7] [also known as 1xEV-DO or high data rate (HDR)], which trades some total system throughput for resource fairness among the active users. In this paper, we present an analysis of the interaction between open-loop antenna diversity and closed-loop multiuser diversity on downlink channels. In Section II, we derive the asymptotic sum rate in the limit of a large number of users with multiple-antenna diversity. We quantitatively evaluate the improvement from multiuser diversity and antennas separately in Section III, along with the impact of finite-user SNR quantization on the average sum rate and the spatial diversity. The more practical PF scheduling is discussed in Section IV, where the focus is on the throughput improvement of twofold receive antenna diversity over that without antenna diversity in a multiuser scenario. Practical issues like channel fading statistics are considered for the total spatial diversity gain. Section V concludes the paper.

II. Asymptotic Sum Rate

A. Multiuser Channel Model

We use a simple downlink model of a cellular packet data system, in which the base station transmitter sends packets to K mobile terminals. There are n_T transmit antennas at the base station and n_R receive antennas at each mobile user for antenna diversity. We assume that the transmission time is divided into consecutive and equal time slots, with the duration of each slot being less than the fading coherence time, and much less than the possible delay constraint of data services, but sufficiently long so that the information-theoretic assumption of infinitely long code block length is meaningful. At each slot t, the packet scheduler at the base station decides to send a packet to user k^* with the largest effective SNR $\gamma_k(t)$ at the receive antenna combiner output

$$k^* = \arg \max_{k=1,\ldots,K} \gamma_k(t) \tag{1}$$

with

$$\gamma_k(t) = \frac{\gamma_s}{n_T} \sum_{j=1}^{n_R} \sum_{i=1}^{n_T} \left| \alpha_{i,j}^{(k)}(t) \right|^2 \tag{2}$$

Paper approved by G. M. Vitetta, the Editor for Equalization and Fading Channels of the IEEE Communications Society. Manuscript received November 26, 2002; revised July 10, 2003 and September 25, 2003.

The authors are with the Mobile and Portable Radio Research Group (MPRG), Bradley Department of Electrical and Computer Engineering, Virginia Polytechnic Institute and State University, Blacksburg, VA 24061 USA (e-mail: jjiang@vt.edu; buehrer@vt.edu; btranter@vt.edu).

Digital Object Identifier 10.1109/TCOMM.2004.823637

where γ_s is the expected SNR at each receive antenna branch for each user, and is assumed a constant independent of the number of transmit antennas. In (2), $\alpha_{i,j}^{(k)}(t)$ represent the ergodic channel fading processes from transmit antenna i to receive antenna j of user k over slot t. Unless specified otherwise, we assume a block-fading channel model with the fading coefficients $\alpha_{i,j}^{(k)}(t)$ being fixed over slot t, and varying independently from slot to slot over time. All $\alpha_{i,j}^{(k)}(t)$ terms are independent and identically distributed (i.i.d.) between each pair of transmit and receive antennas, which assumes that antenna elements are spaced sufficiently with respect to the angle spread. This model presupposes that the signal bandwidth is sufficiently narrow so that the channel fading processes can be assumed flat in frequency. It also assumes that the average total transit power is fixed and equally split over n_T transmit antennas. For simplification, we assume that perfect and instantaneous user channel SNR feedback exists between each transmitter–receiver pair. Also for antenna diversity, we assume that the effective user SNRs, after coherent combing, conforms to (2). However, from the orthogonal design for the space–time codes [8], no "full rate" complex orthogonal design exists for n_T greater than two, for which only the fractional rates are achievable (see [8]).

At slot t, we define the maximum SNR among the K users as

$$\gamma(t) \triangleq \max_{k=1,\ldots,K} \gamma_k(t). \tag{3}$$

Under the assumption of symmetric user channels with i.i.d. SNRs over each slot, and according to the order statistics for i.i.d. continuous random variables [9], the cumulative distribution function (cdf) of γ at any slot is

$$Y(\gamma) = (F(\gamma))^K \tag{4}$$

and the probability density function (pdf) of γ is

$$y(\gamma) = \begin{cases} K \cdot f(\gamma) \cdot F(\gamma)^{K-1}, & \gamma > 0 \\ 0, & \text{otherwise} \end{cases} \tag{5}$$

where $f(\cdot)$ and $F(\cdot)$ are the pdf and cdf of the i.i.d. user SNRs γ_k, respectively. In (4) and (5), the slot index is dropped due to the time independence of the statistics. We define the average sum rate of the channel with the $n_T n_R$-fold antenna diversity and K-fold multiuser diversity as

$$C_{n_T n_R}^K \triangleq \int_0^\infty \log_2(1+\gamma) \cdot y(\gamma)\, d\gamma \tag{6}$$

in bits/second/Hertz. This is the expected achievable sum rate, given the effective user SNRs in (2). Under the assumption of the perfect and instantaneous transmitter knowledge of user CQI in (2), so that greedy scheduling and rate adaptation can be performed at the transmitter, the average sum rate in (6) is bounded away from zero. Throughout this paper, we use the average sum rate metric to evaluate the spatial diversity of the system. We first derive the asymptotic multiuser diversity in the limit of a large number of users, i.e., as $K \to \infty$, in the remainder of this section.

To calculate the limiting distribution of the γ in (3) as $K \to \infty$, we use [3, Lemma 2], which we restate below as *Lemma 1*.

Lemma 1: Let $z_1, \ldots, z_K$ be i.i.d. random variables with a common cdf $F(\cdot)$ and pdf $f(\cdot)$ satisfying that $F(\cdot)$ is less than one for all finite z and is twice differentiable for all z, and is such that

$$\lim_{z\to\infty} \left[\frac{1-F(z)}{f(z)}\right] = c > 0 \tag{7}$$

for some constant c. Then

$$\max_{1\le k\le K} z_k - l_K$$

converges in distribution to a limiting random variable with cdf

$$\exp(-e^{-x/c}).$$

In the above, l_K is given by $F(l_K) = 1 - 1/K$.

Lemma 1 states that the maximum of K such i.i.d. random variables grows like l_K as $K \to \infty$.

B. Symmetric Rayleigh Fading

With the i.i.d. Rayleigh fading channels, γ_k in (2) is a chi-square random variable with $2n_T n_R$ degrees of freedom. Define $n \triangleq n_T n_R - 1$, the pdf and cdf of γ_k are [10], respectively

$$f(\gamma_k) = \frac{1}{(n)!(\gamma_s/n_T)^{n_T n_R}} \gamma_k^n e^{-\frac{\gamma_k}{\gamma_s/n_T}}, \quad \gamma_k > 0 \tag{8}$$

$$F(\gamma_k) = 1 - e^{-n_T\gamma_k/\gamma_s} \sum_{m=0}^{n} \frac{(n_T\gamma_k/\gamma_s)^m}{m!}, \quad \gamma_k > 0. \tag{9}$$

We can easily see that

$$\lim_{\gamma_k\to\infty} \frac{1-F(\gamma_k)}{f(\gamma_k)} = \frac{\gamma_s}{n_T} = c_1 > 0. \tag{10}$$

Solving for l_K from *Lemma 1*, we have

$$l_K = \begin{cases} \frac{\gamma_s}{n_T} \ln K = \gamma_s \ln K, & n_T = n_R = 1 \\ \frac{\gamma_s}{n_T} \ln K + O(\ln\ln K), & \text{otherwise.} \end{cases} \tag{11}$$

Therefore, with i.i.d. Rayleigh fading and for a large number of users, the maximum equivalent SNR γ grows like l_K in (11), which is a function of the number of transmit antennas n_T and the number of users K for the fixed average total transmit power, and is independent of the number of receive antennas n_R. The asymptotic sum rate as $K \to \infty$ can, therefore, be approximated by

$$\lim_{K\to\infty} C_{n_T n_R}^K = \log_2(1+l_K) \approx \log_2\left(1 + \frac{\gamma_s}{n_T}\ln K\right). \tag{12}$$

Fig. 1 shows the numerical evaluation of the average sum rate $C_{n_T n_R}^K$ for the cases of $n_T, n_R = 1, 2$, and 4. We see the surprising result that with multiple users ($K > 1$), the average sum rate with transmit diversity is lower than that without transmit diversity for all cases of $n_R = 1, 2$, and 4, although the opposite is true for the single-user cases. This result is contrary to what is commonly observed over a single wireless link, where transmit diversity always improves link performance in fading. An intuitive explanation for the difference is that for fixed average transmit power, transmit diversity reduces the variation in the received signal power, which is exploited by the greedy scheduler for multiuser diversity. The same is true for receive diversity, but the array gain from coherent receive combing more than compensates for the loss of multiuser diversity. Therefore, care should be exercised in employing open-loop antenna diversity, which may improve single-link performance, but can also degrade system-level performance in the presence of greedy scheduling. We note from Fig. 1 that in order for the $n_T = n_R = 1$ case to outperform the cases of $n_T = n_R = 2$ and $n_T = n_R = 4$, the minimum numbers of users required are

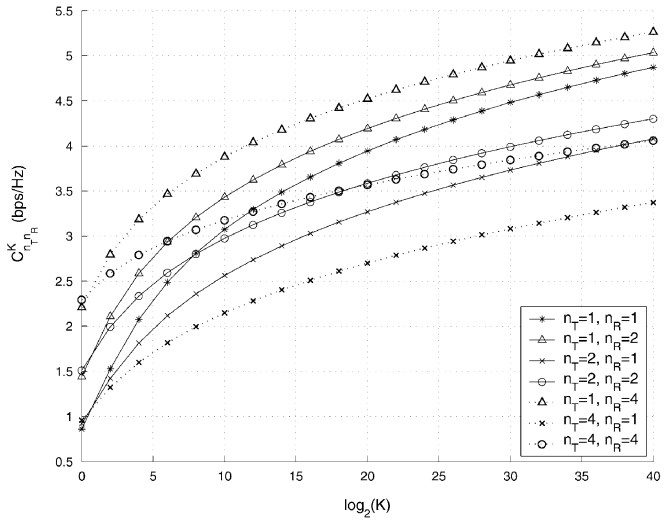

Fig. 1. Average sum rate under i.i.d. flat Rayleigh fading with $\gamma_s = 0$ dB.

about $2^8 = 256$ and $2^{12} = 4096$, respectively. Consistent with (12), for large K, there is an approximate 1 b/s/Hz sum-rate increase for every 3-dB increase in γ_s or a half of n_T. Finally, it is worth noting that although the asymptotic sum rate in (12) is independent of the number of receive antennas, this asymptote is approached at a very slow rate in the number of users, even more so for large n_T.

C. Symmetric Rician Fading

For the i.i.d. Rician fading channels, γ_k in (2) is a noncentral chi-square random variable with $2n_Tn_R$ degrees of freedom. Define $n \triangleq n_Tn_R - 1, \sigma^2 \triangleq 1/(2(1+K_r))$, and $s^2 \triangleq K_rn_Tn_R/(1+K_r)$, where K_r is the Rice factor for all users, the pdf and cdf of γ_k are [10], respectively

$$f(\gamma_k) = \frac{n_T}{2\sigma^2\gamma_s}\left(\frac{n_T\gamma_k/\gamma_s}{s^2}\right)^{\frac{n}{2}} e^{-\frac{s^2+n_T\gamma_k/\gamma_s}{2\sigma^2}} \times I_n\left(\frac{s\sqrt{n_T\gamma_k/\gamma_s}}{\sigma^2}\right), \quad \gamma_k > 0 \tag{13}$$

$$F(\gamma_k) = 1 - e^{-\frac{s^2+n_T\gamma_k/\gamma_s}{2\sigma^2}} \sum_{m=0}^{\infty}\left(\frac{s}{\sqrt{n_T\gamma_k/\gamma_s}}\right)^m \times I_m\left(\frac{s\sqrt{n_T\gamma_k/\gamma_s}}{\sigma^2}\right) - e^{-\frac{s^2+n_T\gamma_k/\gamma_s}{2\sigma^2}} \sum_{m=1}^{n}\left(\frac{\sqrt{n_T\gamma_k/\gamma_s}}{s}\right)^m \times I_m\left(\frac{s\sqrt{n_T\gamma_k/\gamma_s}}{\sigma^2}\right), \quad \gamma_k > 0 \tag{14}$$

where $I_n(\cdot)$ is the nth-order modified Bessel function of the first kind. The tails of the cdf and pdf of γ_k can be approximated, respectively, by

$$f(\gamma_k) \sim \frac{n_T}{\gamma_s}\frac{s^{-n-\frac{1}{2}}}{2\sigma\sqrt{2\pi}}\left(\frac{n_T\gamma_k}{\gamma_s}\right)^{\frac{n}{2}-\frac{1}{4}} e^{-\frac{(\sqrt{n_T\gamma_k/\gamma_s}-s)^2}{2\sigma^2}}$$

$$1 - F(\gamma_k) \sim \frac{\sigma}{\sqrt{2\pi}}s^{-n-\frac{1}{2}}\left(\frac{n_T\gamma_k}{\gamma_s}\right)^{\frac{n}{2}-\frac{1}{4}} e^{-\frac{(\sqrt{n_T\gamma_k/\gamma_s}-s)^2}{2\sigma^2}}.$$

These approximations are in the sense that the ratio of the left- and right-hand sides approaches 1 as $\gamma_k \to \infty$. Hence

$$\lim_{\gamma_k\to\infty}\left[\frac{1-F(\gamma_k)}{f(\gamma_k)}\right] = \frac{2\sigma^2\gamma_s}{n_T} = \frac{\gamma_s}{n_T(1+K_r)} = c_2 > 0. \tag{15}$$

By solving $F(l_K) = 1 - 1/K$, we have

$$l_K = \frac{\gamma_s}{n_T}(s + \sqrt{2\sigma^2\ln K})^2 + O(\ln\ln K) = \frac{\gamma_s}{n_T}\left(\sqrt{\frac{1}{1+K_r}\ln K} + \sqrt{\frac{K_r}{1+K_r}n_Tn_R}\right)^2 + O(\ln\ln K). \tag{16}$$

According to *Lemma 1*, for i.i.d. Rician fading, the maximum equivalent SNR γ grows like l_K in (16) as $K \to \infty$. For the fixed average total transmit power, l_K depends on the number of users, the Rice factor, and both the number of transmit and the number of receive antennas. This differs from that of i.i.d. Rayleigh fading in (11), where l_K is independent of the number of receive antennas. In fact, (16) can be viewed as a generalization of (11) for $K_r > 0$ and $n > 1$. Equations (11) and (16) reduce to those in [3] for $n_T = n_R = 1$ and $\gamma_s = 0$ dB. Similarly, we can have the asymptotic sum rate approximated by

$$\lim_{K\to\infty} C^K_{n_Tn_R} = \log_2(1+l_K) \approx \log_2\left(1 + \frac{\gamma_s}{n_T}\left(\sqrt{\frac{1}{1+K_r}\ln K} + \sqrt{\frac{K_r}{1+K_r}n_Tn_R}\right)^2\right). \tag{17}$$

This is plotted in Fig. 2 for $K = 2^{40}$ and $n_T, n_R = 1, 2$, and 4. We see that the approximate asymptotic sum rate goes up as we increase n_R or decrease n_T with the other term remaining fixed. It also decreases as the Rice factor K_r increases at sufficiently large K_r. This is due to the reduced potential channel diversity gain with increased K_r. As the channel approaches an additive white Gaussian noise (AWGN) channel about the mean SNR γ_sn_R with $K_r \to \infty$, (17) can be further approximated by

$$\lim_{K\to\infty, K_r\to\infty} C^K_{n_Tn_R} \approx \log_2(1+\gamma_sn_R) \tag{18}$$

which is independent of n_T. This trend is shown in Fig. 2 with K_r extended to 30 dB.

We conclude this section by pointing out that in an i.i.d. flat Rayleigh fading environment with more than one user, the orthogonal transmit antenna diversity gain is negative, in that the average sum rate is less than that without transmit diversity in the presence of greedy scheduling. In the limit of $K \to \infty$, the maximum effective SNR γ is inversely proportional to the number of transmit antennas and independent of the number of receive antennas. In the corresponding Rician fading environment, both the number of transmit and the number of receive antennas impact the asymptotic sum rate as $K \to \infty$, with negative gain from transmit diversity and positive gain from receive antennas. However, as the Rice factor becomes sufficiently large

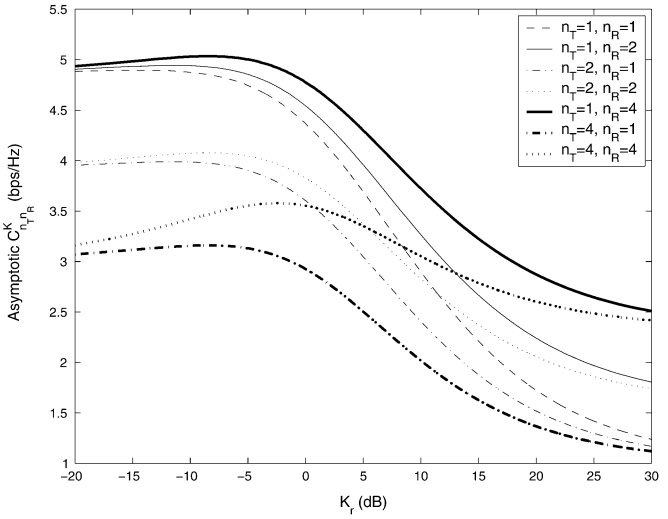

Fig. 2. Approximate asymptotic sum rate for $K = 2^{40}$ users under i.i.d. flat Rician fading with $\gamma_s = 0$ dB.

and the channel approaches an AWGN channel, only the positive power gain from the coherent receive antenna combining remains.

III. Antenna Diversity and Multiuser Diversity

We numerically evaluate the average sum-rate improvement from the antenna and the multiuser diversity separately for a finite number of users. For simplicity, we restrict ourselves to symmetric flat Rayleigh fading channels. We define the antenna improvement as the percentage increase of the average sum rate relative to the single-antenna case of $n_T = n_R = 1$ in a system of K users

$$I_a \triangleq \frac{C^K_{n_T n_R} - C^K_{11}}{C^K_{11}} \tag{19}$$

and the multiuser diversity improvement as the percentage increase of the average sum rate relative to the single-user case

$$I_u \triangleq \frac{C^K_{n_T n_R} - C^1_{n_T n_R}}{C^1_{n_T n_R}}. \tag{20}$$

Figs. 3(a) and (b) illustrate the antenna improvement I_a versus the number of users K at an average SNR of $\gamma_s = 0$ dB, and I_a versus γ_s with $K = 1, 64$, and 2^{40} users, respectively, both for the cases of $n_T, n_R = 1, 2$, and/or 4. The zero-level reference is for the case of $n_T = n_R = 1$. In Fig. 3(a), the $n_T = 2$ and 4 cases have less antenna improvement than the corresponding $n_T = 1$ case when there is more than one user, and the antenna improvement decreases as K increases, and becomes saturated at sufficiently large K. This trend is more pronounced for the cases with transmit diversity only. In Fig. 3(b), we note that in all cases, the improvement of the receive antennas of $n_T = 1$ and $n_R = 4$ decreases with γ_s and remains positive, and the improvement of the transmit antennas of $n_T = 4$ and $n_R = 1$ increases with γ_s consistently at a lower percentage level.

Figs. 4(a) and (b) depict the multiuser diversity improvement I_u versus K at $\gamma_s = 0$ dB, and I_u versus γ_s with $K = 64$ and 2^{40} users, respectively, also both for the cases of $n_T, n_R = 1$ or 2 and/or 4. The plots show that I_u monotonically increases

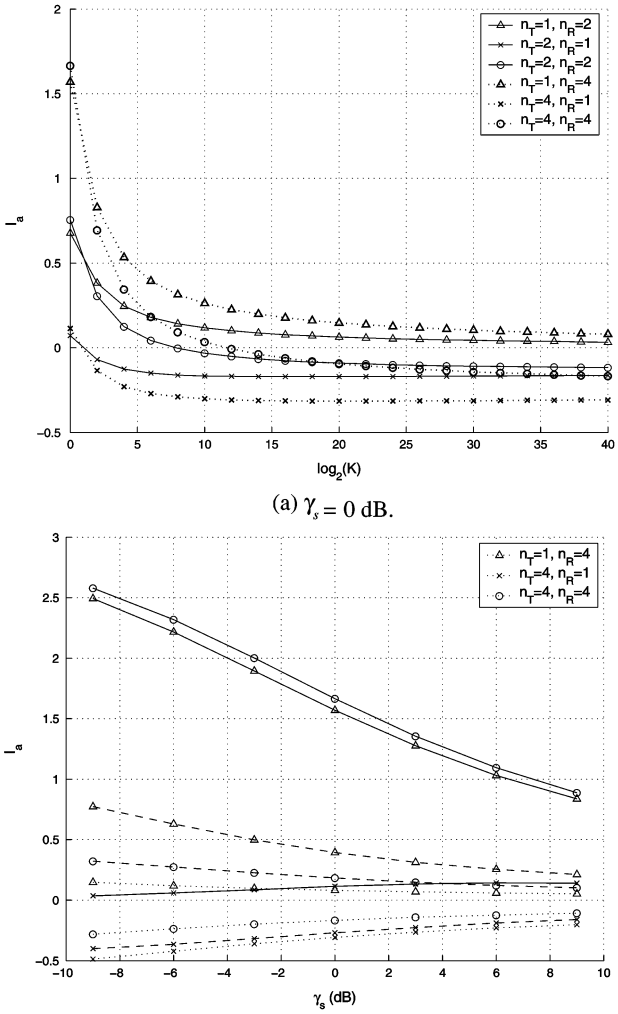

(a) $\gamma_s = 0$ dB.

(b) Solid curves: K =1; dashed curves: K = 64; dotted curves: $K = 2^{40}$.

Fig. 3. Antenna improvement in i.i.d. flat Rayleigh fading. (a) $\gamma_s = 0$ dB. (b) Solid curves: $K = 1$; dashed curves: $K = 64$; dotted curves: $K = 2^{40}$.

with K, but monotonically decreases with γ_s, both at percentage levels much higher than those in Fig. 3 for a sufficient number of users. In all cases, the improvement of multiuser diversity is positive. Comparing Fig. 3 with Fig. 4, we see that average sum-rate improvement is dominated by the multiuser diversity in a network, in most cases with a finite number of users, e.g., $K > 64$ for $n_T, n_R = 1$ or 4.

In evaluating the improvement of antenna and multiuser diversity in terms of the relative increase of the average sum rate, we have assumed the instantaneous and perfect feedback of a continuum of SNR values to the base station. We have also assumed that over each slot, the sum rate can be achieved physically at those SNR values by some powerful coding and modulation techniques. We now evaluate the effect of finite channel SNR quantization on the antenna and multiuser diversity improvement. We still retain the other assumptions given above, except that the effective SNRs γ_k are now quantized into one of $Q+1$ values, ranked in an ascending order from zero as follows:

$$\gamma_{Q,k} \in \{0, \hat{\gamma}_0, \hat{\gamma}_1, \ldots, \hat{\gamma}_{Q-1}\}, \quad k = 1, \ldots, K. \tag{21}$$

The quantization is to the lower value over each interval of SNR in (21), with 0 and $\hat{\gamma}_{Q-1}$ being the lower and upper limit, re-

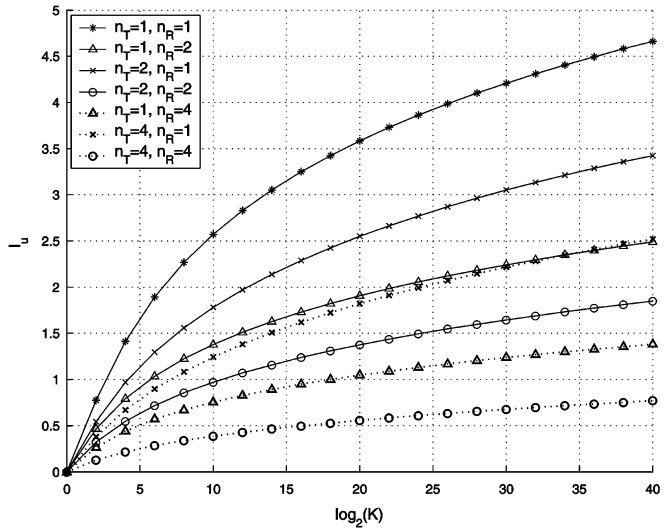

(a) $\gamma_s = 0$ dB.

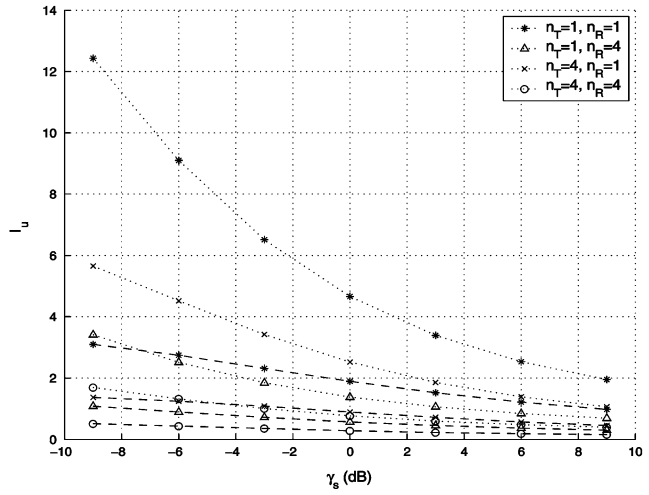

(b) dashed curves: $K = 64$; dotted curves: $K = 2^{40}$.

Fig. 4. Multiuser diversity improvement in i.i.d. flat Rayleigh fading. (a) $\gamma_s = 0$ dB. (b) Dashed curves: $K = 64$; dotted curves: $K = 2^{40}$.

spectively. The probability mass function (pmf) of the discrete random variables $\gamma_{Q,k}$ can be calculated as

$$\begin{aligned} p(\gamma_{Q,k}) &= \left(\int_0^{\hat{\gamma}_0} f(\gamma_k)\,d\gamma_k\right)\cdot\delta[\gamma_{Q,k}] \\ &\quad + \sum_{i=0}^{Q-2}\left(\int_{\hat{\gamma}_i}^{\hat{\gamma}_{i+1}} f(\gamma_k)\,d\gamma_k\right) \\ &\quad \cdot\delta[\gamma_{Q,k}-\hat{\gamma}_i] + \left(\int_{\hat{\gamma}_{Q-1}}^{\infty} f(\gamma_k)\,d\gamma_k\right) \\ &\quad \cdot\delta[\gamma_{Q,k}-\hat{\gamma}_{Q-1}] \\ &= F(\hat{\gamma}_0)\cdot\delta[\gamma_{Q,k}] + \sum_{i=0}^{Q-2}(F(\hat{\gamma}_{i+1})-F(\hat{\gamma}_i)) \\ &\quad \cdot\delta[\gamma_{Q,k}-\hat{\gamma}_i] + (1-F(\hat{\gamma}_{Q-1}))\cdot\delta[\hat{\gamma}_{Q,k}-\hat{\gamma}_{Q-1}] \end{aligned} \tag{22}$$

where $\delta[n-m]$ is the Kronecker delta function. The cdf of $\gamma_{Q,k}$ is, therefore, the stair function

$$\begin{aligned} P(\gamma_{Q,k}) &= F(\hat{\gamma}_0)\cdot u(\gamma_{Q,k}) + \sum_{i=0}^{Q-2}(F(\hat{\gamma}_{i+1})-F(\hat{\gamma}_i)) \\ &\quad \cdot u(\gamma_{Q,k}-\hat{\gamma}_i) + (1-F(\hat{\gamma}_{Q-1}))\cdot u(\gamma_{Q,k}-\hat{\gamma}_{Q-1}) \\ &= \begin{cases} F(\hat{\gamma}_0), & 0 \le \gamma_{Q,k} < \hat{\gamma}_0 \\ F(\hat{\gamma}_{i+1}), & \hat{\gamma}_i \le \gamma_{Q,k} < \hat{\gamma}_{i+1}, i = 0,\ldots,Q-2 \\ 1, & \gamma_{Q,k} \ge \hat{\gamma}_{Q-1} \end{cases} \end{aligned} \tag{23}$$

where $u(x-x_0)$ is the unit step function. According to the order statistics for i.i.d. discrete random variables [9], the cdf and pmf of the maximum quantized SNR γ_Q

$$\gamma_Q \triangleq \max_{k=1,\ldots,K}\gamma_{Q,k}$$

are, respectively

$$Y_Q(\gamma_Q) = (P(\gamma_Q))^K \tag{24}$$

$$\begin{aligned} y_Q(\gamma_Q) &= Y_Q(0)\cdot\delta[\gamma_Q] + (Y_Q(\hat{\gamma}_0)-Y_Q(0)) \\ &\quad \cdot\delta[\gamma_Q-\hat{\gamma}_0] + \sum_{i=1}^{Q-1}(Y_Q(\hat{\gamma}_i)-Y_Q(\hat{\gamma}_{i-1}))\cdot\delta[\gamma_Q-\hat{\gamma}_i] \\ &= F(\hat{\gamma}_0)^K\cdot\delta[\gamma_Q] + \sum_{i=0}^{Q-2}(F(\hat{\gamma}_{i+1})^K - F(\hat{\gamma}_i)^K) \\ &\quad \cdot\delta[\gamma_Q-\hat{\gamma}_i] + (1-F(\hat{\gamma}_{Q-1})^K)\cdot\delta[\gamma_Q-\hat{\gamma}_{Q-1}]. \end{aligned} \tag{25}$$

The average sum rate with Q nonzero-SNR quantization levels can be calculated from

$$\begin{aligned} D^K_{n_T n_R} &\triangleq \sum_{i=0}^{Q-1}\log_2(1+\hat{\gamma}_i)\cdot y_Q(\hat{\gamma}_i) \\ &= \sum_{i=0}^{Q-2}\log_2(1+\hat{\gamma}_i)\cdot(F(\hat{\gamma}_{i+1})^K - F(\hat{\gamma}_i)^K) \\ &\quad + \log_2(1+\hat{\gamma}_{Q-1})\cdot(1-F(\hat{\gamma}_{Q-1})^K). \end{aligned} \tag{26}$$

Fig. 5 illustrates $D^K_{n_T n_R}$ with $Q = 8$ uniform SNR quantization levels (in decibels), using $\hat{\gamma}_0 = -11.5$ dB and $\hat{\gamma}_{Q-1} = 9.5$ dB in i.i.d. flat Rayleigh fading with $\gamma_s = 0$ dB for the cases of $n_T, n_R = 1, 2$, and 4. For $Q = 8$, $D^K_{n_T n_R}$ in (26) is above 78% of the value of $C^K_{n_T n_R}$ in (6). For the cases of $Q = 32$ and 16 (not shown in Fig. 5), $D^K_{n_T n_R}$ is above 94% and 89%, respectively, of $C^K_{n_T n_R}$ for $n_T, n_R = 1$ or 2, and above 85% and 85%, respectively, of $C^K_{n_T n_R}$ for $n_T, n_R = 1$ or 4. Comparing Fig. 5 with Fig. 1, we note that at fixed quantization limits, the average sum rate with SNR quantization is reduced more by receive diversity. The reason is given below.

In the process of user SNR quantization, γ_k greater than $\hat{\gamma}_{Q-1}$ will be quantized to $\hat{\gamma}_{Q-1}$ according to (21), so the maximum SNR increase above γ_{Q-1} contributes no sum-rate increase. We define the relative probability of γ greater than $\hat{\gamma}_{Q-1}$ as the SNR clipping rate

$$\begin{aligned} R_{\text{clip}} &\triangleq \frac{\Pr\{\gamma > \hat{\gamma}_{Q-1}\}}{\Pr\{\gamma > \hat{\gamma}_0\}} = \frac{1-Y(\hat{\gamma}_{Q-1})}{1-Y(\hat{\gamma}_0)} \\ &= \frac{1-F(\hat{\gamma}_{Q-1})^K}{1-F(\hat{\gamma}_0)^K} \end{aligned} \tag{27}$$

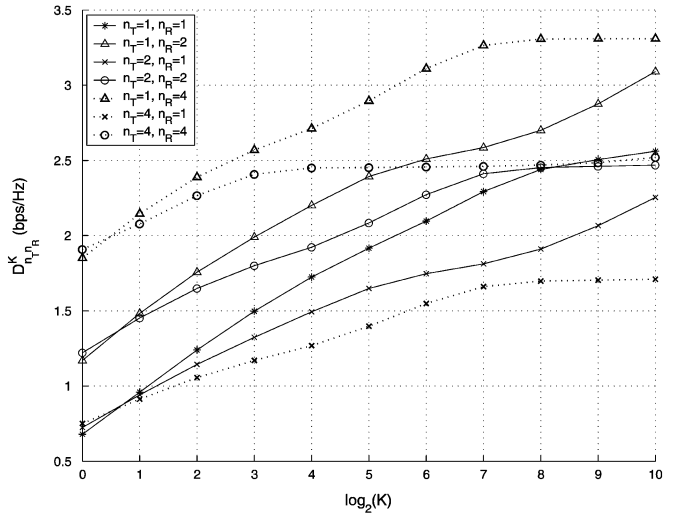

Fig. 5. Average sum rate in i.i.d. flat Rayleigh fading at $\gamma_s = 0$ dB. $\hat{\gamma}_i$ is uniformly spaced (in decibels) over $[-11.5\,9.5]$ dB with $Q = 8$.

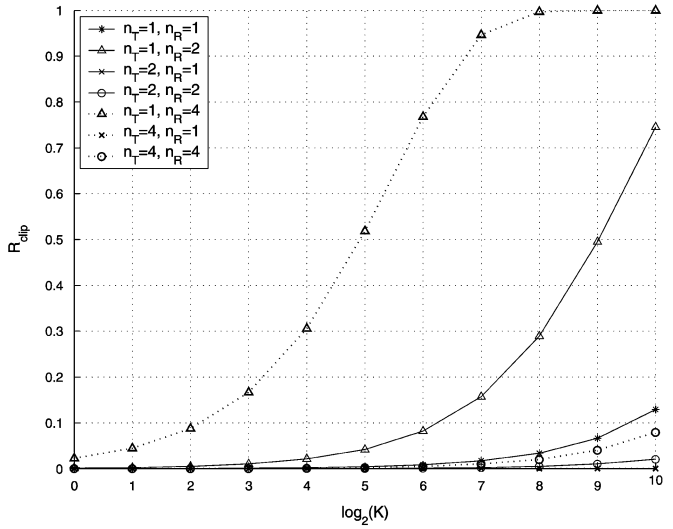

Fig. 6. Clipping rate in i.i.d. flat Rayleigh fading for $\hat{\gamma}_0 = -11.5$ dB and $\hat{\gamma}_{Q-1} = 9.5$ dB at $\gamma_s = 0$ dB.

with $0 < R_{\text{clip}} < 1$, and $\lim_{K\to\infty} R_{\text{clip}} = 1$. In a large network employing antenna diversity, for power-efficiency purposes, we want the SNR clipping rate to be as small as possible, given the SNR quantization. The clipping rate R_{clip} is plotted in Fig. 6 with the same SNR limits above, at $\gamma_s = 0$ dB for the cases of $n_T, n_R = 1, 2$, and 4. As shown in Fig. 6, the SNR clipping rate can be nontrivial, even at $\gamma_s = 0$ dB, for a modest number of users. For the case of $n_T = 1$ and $n_R = 2$, and the number of users $K = 512$, there is about a 50% probability that the maximum received SNR will exceed the 9.5-dB upper limit at $\gamma_s = 0$ dB. For $n_T = 1$ and $n_R = 4$, the same clipping rate occurs at K less than 32. As the maximum effective SNR increases, the SNR clipping rate increases. This suggests an adaptive SNR quantization scheme, which accounts for the expectation of the spatial diversity improvement. It should be noted that the clipping rate of $n_T = 1$ and $n_R = 4$ at $\gamma_s = 0$ dB is the same as that of $n_T = 2$ and $n_R = 2$ at $\gamma_s = 3$ dB. This is due to the same cdf $F(\gamma_k)$ in (9) for the two cases, which leads to the same clipping rate R_{clip} in (27).

IV. PF Scheduling and Its Implication on Spatial Diversity

In the previous sections, we assumed that the maximum total throughput is achieved with the aid of a greedy and channel-aware packet scheduler at the base station. We pointed out that this scheduler is optimal in the sense that it achieves the maximum total throughput given the signaling schemes in this paper. However, in real systems, packet scheduling is constrained by the maximum application-delay tolerance, though this delay requirement is much more relaxed for packet data services than for the voice or streaming video services. The scheduling scheme also must consider the fairness among multiple users for the service. For this reason, the PF scheduling was proposed in [6] for the IS-856 downlink packet scheduling, and its performance limitations and improvement were shown in [3]. The resource fairness is maintained by providing a fair sharing of transmission time proportional to the past throughputs of users. With PF scheduling, at each slot t, user k feeds back to the base station a requested data rate $R_k(t)$, which is supportable by its current SNR $\gamma_k(t)$. Here again, an instantaneous and error-free rate feedback is assumed. The scheduler assigns the slot t to the user k^*, which has the largest ratio

$$\frac{R_k(t)}{T_k(t)}$$

among all active users, where $T_k(t)$ is the kth user's average throughput in a past window of length W_c, and is updated slot-wise according to

$$T_k(t+1) = \begin{cases} \left(1 - \frac{1}{W_c}\right) T_k(t) + \frac{1}{W_c} R_k(t), & k = k^* \\ \left(1 - \frac{1}{W_c}\right) T_k(t), & k \neq k^* \end{cases}$$

where W_c is the time scale of interest and is constrained by the maximum delay tolerance. In IS-856, W_c is about 1.67 s. For symmetric user channels with $W_c \to \infty$, we have $T_k = T$ for $k = 1, \ldots, K$. Therefore, the greedy scheduling can be viewed as a special case of the PF scheduling for infinite window length and symmetric user channels. Results from both the simulation [6] and the HDR system field testing [11], [12] have shown that the two-fold receive antenna diversity can lead to double the physical-layer average total throughput in some slow-to-medium-fading environments. In this section, we present the numerical throughput improvement with two receive antennas over a single receive antenna in a multiuser scenario, and we focus on the HDR system downlink applications. As before, we assume that the user channel fading is symmetric. However, instead of the i.i.d. block-fading model, we assume that the fading processes are ergodic with continuous fading variations across slots, and have low-to-medium Doppler rates corresponding to pedestrian-to-low-vehicular speed.

The performance of the PF scheduling is affected by both the channel-fading statistics and the number of active users. Figs. 7(a) and (b) plot the average total throughput for the 1.5-Hz Doppler Rician fading with a Rice factor $K_r = 10$ and the 55.6-Hz Doppler Rayleigh fading channels, respectively, by using the mapping table in [11] for the SNR-to-data-rate mapping without the hybrid automatic repeat request (H-ARQ) on the physical layer. The adaptive data rate is achieved on a single 1.25-MHz physical channel. The mapping is shown in Table I.

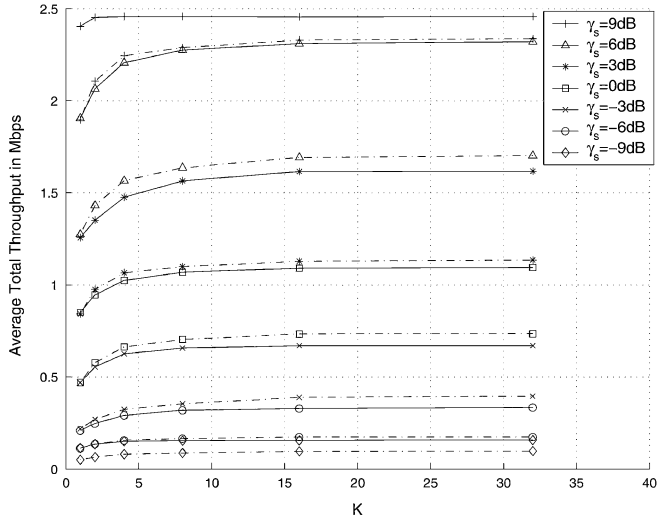

(a) In i.i.d. 1.5 Hz-Doppler flat Rician (K_r =10) fading over 8000 slots with 16.7 ms per slot and W_c =100 slots.

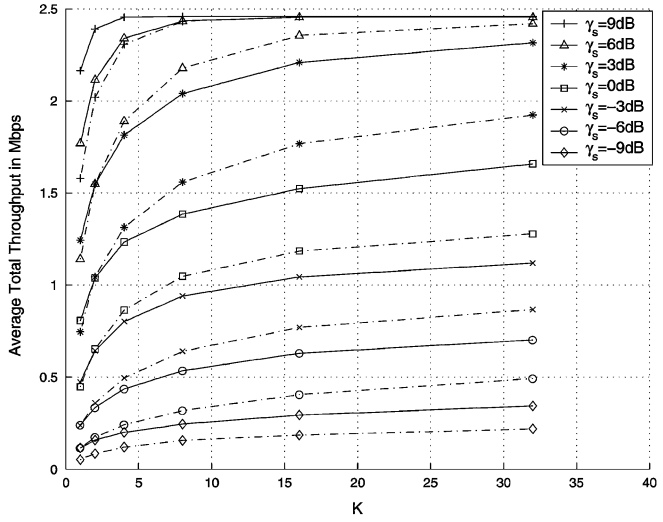

(b) In i.i.d. 55.6 Hz-Doppler flat Rayleigh fading over 2000 slots with 8.3 ms per slot and W_c= 200 slots.

Fig. 7. Average total throughput using PF scheduling with γ_s from 9 dB to -9 dB in a step size of 3 dB from top to bottom. Solid curves: $n_T = 1$ and $n_R = 2$; dash-dotted curves: $n_T = 1$ and $n_R = 1$. (a) In i.i.d. 1.5-Hz Doppler flat Rician ($K_r = 10$) fading over 8000 slots with 16.7 ms per slot and $W_c = 100$ slots. (b) In i.i.d. 55.6-Hz Doppler flat Rayleigh fading over 2000 slots with 8.3 ms per slot and $W_c = 200$ slots.

For simplicity purposes, we replace variable-length packet scheduling with fixed-length packet scheduling over each slot of about 1.67 ms. As we can see from these figures, the higher fading rate and the larger fading dynamics are beneficial from the total throughput point of view, but they are subject to higher receive SNR clipping rates, which is especially pronounced at high average SNR regimes. Compared with Fig. 1, the spectral efficiency is more modest in Fig. 7. In addition to the SNR quantization, the lower spectral efficiency also comes as a price for the resource fairness over a window length W_c of about 1.67 s. In Fig. 7(a), for the slow-fading case with a strong line-of-sight component, the spectral efficiency suffers more due to limited multiuser diversity over W_c. Plots in Figs. 7(a) and (b) also show that a doubling of throughput with 100% user average SNR increase cannot always be expected, since

TABLE I
SNR-TO-DATA-RATE MAPPING WITHOUT H-ARQ

Data Rate Index (4 bits)	Data Rate (Kbps)	$\gamma_k(t)$ Threshold (dB) (5/3 ms per slot)
0	0	$\gamma_k(t) < -11.5$
1	38.4	$-11.5 \le \gamma_k(t) < -9.0$
2	76.8	$-9.0 \le \gamma_k(t) < -6.5$
3	153.6	$-6.5 \le \gamma_k(t) < -3.0$
4	307.2	$-3.0 \le \gamma_k(t) < -0.5$
5	614.4	$-0.5 \le \gamma_k(t) < 2.0$
6	921.6	$2.0 \le \gamma_k(t) < 4.0$
7	1228.8	$4.0 \le \gamma_k(t) < 7.0$
8	1843.2	$7.0 \le \gamma_k(t) < 9.5$
9	2457.6	≥ 9.5

both the user fading statistics and the number of users vary in a multiuser network. Generally, the higher improvement can be expected under the conditions of the lower average SNR γ_s, the smaller fading variation, or the smaller number of active users. The first condition is due to the low SNR approximation of the achievable rate by

$$C = \log_2(1+\rho) = (\log_2 e)\cdot \ln(1+\rho) \approx \rho \log_2 e$$

in bits/second/Hertz for SNR $\rho \ll 1$. Therefore, in the vicinity of very low SNR, a 3-dB increase in SNR does double the throughput. The last two conditions are related to limited multiuser diversity via PF scheduling with finite window length. In those cases, the receive antenna diversity improvement can become more apparent, given that the potential channel diversity is not fully exploited via multiuser diversity.

V. CONCLUSION AND FUTURE RESEARCH WORK

In a large data network of multiple users, multiuser diversity can greatly increase system throughput. We have shown that under greedy packet scheduling, open-loop transmit antenna diversity over each point-to-point wireless link can have an adverse effect on the total system throughput. The asymptotic sum-rate analysis also shows that receive antenna diversity can be a waste of resources in the limit of a large number of users for the i.i.d. Rayleigh fading channels. That is, for a network with a large number of users, the performance gain from receive antenna diversity can be minimal and should be evaluated to assess whether it warrants the additional implementation cost and complexity. Attention should also be paid to prevent the nonnegligible received SNR clipping rate, which can substantially reduce the power efficiency in high SNR regions. On the other hand, in the application environments where the potential multiuser diversity gain is constrained by fairness concerns, benign fading channels with insufficient scattering, strong light-of-sight signal components, or a slow fading rate,

the implementation of receive antenna diversity may be justified. In this paper, we have not considered diversity techniques in other forms, for instance, frequency diversity in the form of maximal-ratio Rake combing, or time diversity in the form of interleaving and error-correction channel coding. The quantitative evaluation of gains from all these diversity techniques and their interaction in a multilink system remains an interesting topic. With CQI at the transmitter, closed-loop antenna diversity can also be exploited. An example is selection transmit diversity, which selects the best among n_T independent transmit antennas for each user using CQI feedback. In our channel model, this is equivalent to greedy scheduling with a single transmit antenna and n_T times the number of users. Therefore, unlike open-loop transmit diversity, selection transmit diversity can improve system throughput with greedy scheduling, although the gains may still be small.

In addition to diversity, multiple transmit antennas can provide spatial multiplexing and improve system throughput with scheduling. An interesting issue for our future research is the evaluation of downlink throughput improvement by using multiple transmit antennas effectively and efficiently. Furthermore, the tradeoff issue between diversity gain and multiplexing gain over multiple-input/multiple-output downlink channels is also an interesting and challenging subject.

ACKNOWLEDGMENT

The authors would like to thank the anonymous reviewers for their insightful comments and suggestions for improving the quality of this paper.

REFERENCES

[1] H. Huang, H. Viswanathan, A. Blanksby, and M. A. Haleem, "Multiple antenna enhancements for a high rate CDMA packet data system," *J. VLSI Signal Processing*, no. 30, pp. 55–69, Jan.-Mar. 2002.

[2] R. Gozali, R. M. Buehrer, and B. D. Woerner, "The impact of multiuser diversity on space–time block coding," *IEEE Commun. Lett.*, vol. 7, pp. 213–215, May 2003.

[3] P. Viswanath, D. N. C. Tse, and R. Laroia, "Opportunistic beamforming using dumb antennas," *IEEE Trans. Inform. Theory*, vol. 48, pp. 1277–1294, June 2002.

[4] R. Knopp and P. Humblet, "Information capacity and power control in single-cell multiuser communications," in *Proc. IEEE Int. Conf. Communications*, Seattle, WA, June 1995, pp. 331–335.

[5] D. N. C. Tse, "Optimal power allocation over parallel Gaussian broadcast channels," in *Proc. IEEE Int. Symp. Information Theory*, Ulm, Germany, June 1997, p. 27.

[6] A. Jalali, R. Padovani, and R. Pankaj, "Data throughput of CDMA-HDR: A high efficiency-high data rate personal communication wireless system," in *Proc. IEEE 50th Vehicular Technology Conf.*, Tokyo, Japan, May 2000, pp. 1854–1858.

[7] *CDMA2000 High Rate Packet Data Air Interface Specification*, TIA/EIA/3GPP2 Standard IS-856/3GPP2 C.S0024, v.3.0, Dec. 2001.

[8] V. Tarokh, H. Jafarkhani, and A. R. Calderbank, "Space–time block codes from orthogonal designs," *IEEE Trans. Inform. Theory*, vol. 45, pp. 1456–1467, July 1999.

[9] H. A. David, *Order Statistics*, 1st ed. New York: Wiley, 1970, pp. 7–13.

[10] J. G. Proakis, *Digital Communications*, 3rd ed. New York: McGraw-Hill, 1995, pp. 41–45.

[11] Y. Jou, "Development in third-generation (3G) CDMA technology," in *Proc. IEEE 6th Int. Symp. Spread Spectrum Techniques, Applications*, vol. 2, Parsippany, NJ, Sept. 2000, pp. 460–464.

[12] *1xEV: 1xEVolution IS-856 TIA/EIA Standard Airlink Overview*, rev. 7.2, Qualcomm, Inc., San Diego, CA, Nov. 2001.

Jing Jiang (S'98) received the B.S. and M.S. degrees in radio engineering with honors from the University of Electronic Science and Technology of China, Chengdu, China, in 1995, and the M.S. degree in communications from Mississippi State University, Mississippi State, MS, in 1998. She is currently working toward the Ph.D. degree at the Bradley Department of Electrical and Computer Engineering, Virginia Polytechnic Institute and State University, Blacksburg (Virginia Tech).

In 1999, she was a Staff Scientist with Adtran, Inc., Huntsville, AL. In the summers of 2000 and 2001, she interned at Lucent Technologies, Whippany, NJ, and Nokia Research Lab, Irving, TX. Her current research interests include network information theory, space–time signal processing, and multiuser packet scheduling.

Ms. Jiang received the Daniel E. Noble Fellowship jointly from the IEEE Vehicular Technology Society and Motorola in 2002.

R. Michael Buehrer (S'89–M'96) is currently an Assistant Professor with the Bradley Department of Electrical and Computer Engineering, Virginia Polytechnic Institute and State University, Blacksburg (Virginia Tech), where he works with the Mobile and Portable Radio Research Group. His current projects include propagation measurement and channel modeling of ultra-wideband (UWB) signals as part of the DARPA NETEX program. Other projects include communication system and receiver design for UWB, multiuser MIMO system design, implementation of direction-finding algorithms on software-defined radio platforms, general software radio research, multiuser detection, spread spectrum, communication system optimization, adaptive antennas, spatial channel modeling, adaptive modulation and coding, and OFDM-based modulation techniques. From 1996–2001, he was with Bell Laboratories—Lucent Technologies, Murray Hill and Whippany, NJ, working in the areas of CDMA receiver design, multiuser detection, adaptive antennas, and spatial channel modeling. He has co-authored more than a dozen journal and 25 conference papers and holds nine patents in the area of wireless communications.

Dr. Buehrer was named Outstanding New Assistant Professor by the Virginia Tech College of Engineering in 2003.

William H. Tranter (S'63–M'68–SM'80–F'85) received the B.S.E.E., M.S.E.E., and Ph.D. degrees from the University of Alabama, Tuscaloosa, in 1964, 1965, and 1970, respectively.

He joined the faculty of the University of Missouri-Rolla in 1969. From 1980 to 1985, he served as Associate Dean of Engineering and he served in that position until his early retirement in 1997. In 1997, he joined the Electrical Engineering faculty of the Virginia Polytechnic Institute and State University, Blacksburg (Virginia Tech), as the Bradley Professor of Communications. He currently serves as Director of Virginia Tech's Mobile and Portable Radio Research Group. His research interests are digital signal processing and computer-aided design of communication systems applied to wireless communications systems. He has authored numerous technical papers and is the co-author of three textbooks: *Principles of Communications: Systems, Modulation and Noise* (New York: Wiley, 2002), *Signals and Systems* (Englewood Cliffs, NJ: Prentice-Hall, 1998), and *Principles of Communication Systems Simulation with Wireless Applications* (Englewood Cliffs, NJ: Prentice-Hall, 2004).

Dr. Tranter was named Schlumberger Professor of Electrical Engineering in 1985 by the University of Missouri–Rolla. He currently serves as Director of Education for the IEEE Communications Society and is a Senior Editor of the IEEE JOURNAL ON SELECTED AREAS IN COMMUNICATIONS. For the past five years, he has served as a member of the Board of Governors of the IEEE Communications Society, and has also served as Vice President—Technical Activities, Director of Journals, and as Editor-in-Chief of the IEEE JOURNAL ON SELECTED AREAS IN COMMUNICATIONS.